Chapter 15
Time Dynamics and Entropy Production to Thermalization in EGOE

In this final chapter, we will consider time evolution of isolated finite many-particle systems with random two-body interactions in presence of a mean-field. As pointed out first by Flambaum [1], results here will be useful in the study of the stability of a quantum computer against quantum chaos. Similarly, as Lea Santos and others have pointed out [2–4], they are important in the study of issues related to thermalization in isolated finite quantum systems. It is also possible to address fidelity and Loschmidt echoes in many-particle quantum systems [5]. We will discuss the available results briefly in the next three sections.

15.1 Time Dynamics in BW and Gaussian Regions in EGOE(1 + 2) and BEGOE(1 + 2)

Let us consider a system of m spinless particles (fermions or bosons) in N sp states with the Hamiltonian consisting of a mean-field [generated by a one-body part $h(1)$] and a random two-body interaction $V(2)$ with strength λ,

$$H = h(1) + \lambda V(2). \tag{15.1}$$

Note that $V(2)$ is represented by EGOE(2) or BEGOE(2) with GOE(1) representation in two-particle space. Say the system is prepared in a state $|k\rangle$ and this is assumed to be an eigenstate of $h(1)$. Then at time $t = 0$,

$$\Psi(t = 0) = |k\rangle = \sum_E C_k^E |E\rangle. \tag{15.2}$$

After time 't', the state changes to $\psi(t)$,

$$\Psi(t) = \big|k(t)\big\rangle = \exp -iHt|k\rangle. \tag{15.3}$$

V.K.B. Kota, *Embedded Random Matrix Ensembles in Quantum Physics*,
Lecture Notes in Physics 884, DOI 10.1007/978-3-319-04567-2_15,

Here we are putting $\hbar = 1$ so that t is in E^{-1} units. Applying Eq. (15.2) will give,

$$\begin{aligned}\Psi(t) = \big|k(t)\big\rangle &= \sum_E C_k^E \exp -iEt|E\rangle \\ &= \sum_{E,f} C_k^E C_f^E \exp -iEt|f\rangle \end{aligned} \tag{15.4}$$

where $|f\rangle$ are the complete set of eigenstates of $h(1)$ with $|k\rangle$ being one of them. Thus, the probability that the state $|k\rangle$ changes to the state $|f\rangle$ is $W_{k\to f}(t)$ where

$$\begin{aligned} W_{k\to f}(t) &= \big|\langle f|\exp -iHt|k\rangle\big|^2 = \big|A_{k\to f}(t)\big|^2; \\ A_{k\to f}(t) &= \sum_E C_k^E C_f^E \exp -iEt. \end{aligned} \tag{15.5}$$

Now, the survival or return probability is

$$W_{k\to k}(t) = \big|A_{k\to k}(t)\big|^2 = \left|\sum_E \big[C_k^E\big]^2 \exp -iEt\right|^2. \tag{15.6}$$

The $A_{k\to k}$ can be written as an integral using the discrete form of the strength function $F_k(E)$,

$$A_{k\to k}(t) = \int F_k(E) \exp -iEt\, dE. \tag{15.7}$$

With H represented by EGOE(1 + 2) [or BEGOE(1 + 2)] and the interaction strength $\lambda > \lambda_c$, level and strength fluctuations follow GOE and hence in this region one can replace to a good approximation $F_k(E)$ by its smoothed form. Thus, the first important results is that in most situations the smoothed form of strength functions determine time evolution in EE. As established in Chaps. 5 and 9, $F_k(E)$ changes from BW to Gaussian form as λ increases from λ_c. With this, we will consider four situations: (i) small 't' limit where we can apply perturbation theory; (ii) BW limit of EGOE(1+2) and BEGOE(1+2); (iii) Gaussian region of EGOE(1+2) and BEGOE(1 + 2); (iv) region intermediate to BW and Gaussian forms for $F_k(E)$. Several of the results for (i)–(iii) were given first by Flambaum and Izrailev [1, 6].

15.1.1 Small 't' Limit: Perturbation Theory

For small 't', we can write $\exp -iEt \simeq [\exp -ih(1)t][\exp -iV(2)t]$. Then,

$$\begin{aligned} A_{k\to k}(t) &= \langle k|\exp -iHt|k\rangle = [\exp -iE_k t]\langle k|\exp -iV(2)t|k\rangle \\ &= [\exp -iE_k t]\langle k|1 - iV(2)t - \big[V(2)\big]^2 t^2/2 + \cdots |k\rangle \\ &\simeq [\exp -iE_k t]\big[1 - \sigma_k^2 t^2/2\big] \simeq \exp\big[-iE_k t - \big(\sigma_k^2 t^2/2\big)\big]. \end{aligned} \tag{15.8}$$

Here, we have used the results $E_k = \langle k|H|k\rangle \simeq \langle k|h(1)|k\rangle$ and $\sigma_k^2 = \langle k|H^2|k\rangle - E_k^2 \simeq \langle k|[V(2)]^2|k\rangle$; see [7] for details. Thus, in the small 't' region we have for the return probability,

$$W_{k\to k}(t) = \exp -\sigma_k^2 t^2. \tag{15.9}$$

Some numerical examples testing Eq. (15.9) are shown in Figs. 15.1a for fermions and 15.1c for boson systems

15.1.2 Breit-Wigner Region

In the BW region with λ, the strength of the two-body interaction, not far from λ_c, the strength function will be of BW form with level and strength fluctuations following GOE. In this situation, replacing $F_k(E)$ by BW form (with spreading width Γ) in Eq. (15.7) we obtain,

$$A_{k\to k}(t) = \int_{-\infty}^{+\infty} \frac{\Gamma}{2\pi[(E-E_k)^2 + \frac{\Gamma^2}{4}]} \exp -iEt\, dE. \tag{15.10}$$

This is nothing but the Fourier transform of the BW function and the result for this is well known [8, 9]. Applying this gives,

$$A_{k\to k}(t) = \exp -\left[iE_k t + \frac{\Gamma}{2}t\right]. \tag{15.11}$$

Therefore, for BW the return probability will follow exponential law,

$$W_{k\to k}(t) \overset{BW\ region}{\longrightarrow} \exp -\Gamma t. \tag{15.12}$$

Note that, when t is in $[\sigma_H]^{-1}$ units, the spreading width Γ will be in σ_H units. Some numerical examples testing Eq. (15.12) are shown in Figs. 15.1b for fermions and d for boson systems. In all the calculations (presented in Figs. 15.1–15.3), the $|k\rangle$ states are the mean-field states obtained by the distributing m particles in the given N sp states. Similarly, the basis state energies E_k are the diagonal matrix elements of H in the m-particle basis states giving $E_k = \langle k|h(1) + \lambda V(2)|k\rangle$. Note that the centroids of the E_k energies are same as that of the eigenvalue (E) spectra but their widths are different. In the calculations E and E_k are zero centered (for each member) and scaled by the spectrum width. In all the calculations, the sp energies are taken as independent Gaussian random variables. In order to calculate ensemble averaged $W_{k\to f}$, for each member at a given time t, $|A_{k\to f}(t)|^2$ are summed over the basis states $|k\rangle$ and $|f\rangle$ in the energy windows $E_k \pm \delta$ and $E_f \pm \Delta$. Then, ensemble averaged $W_{k\to f}(t)$ for fixed k is obtained by binning. In Fig. 15.1, results are shown for $W_{k\to k}(t)$ for $E_k = 0$ with $\delta = \Delta = 0.005$.

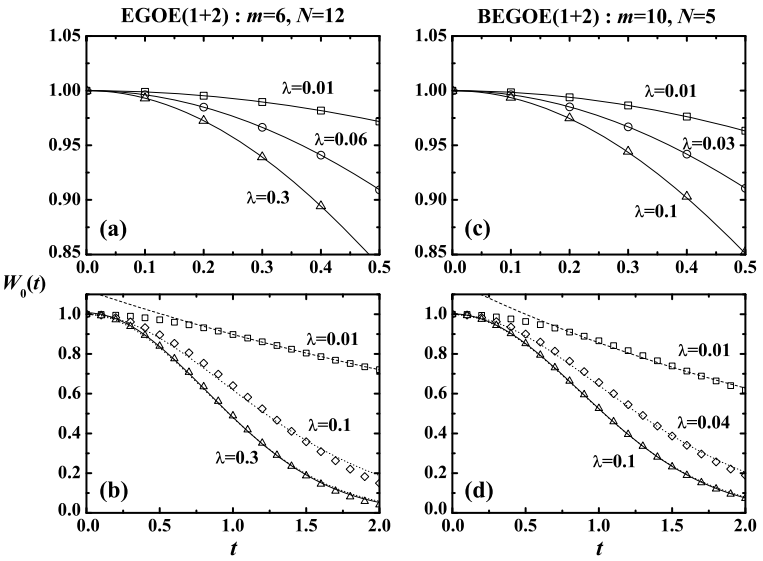

Fig. 15.1 Results for different values of λ for the return probability $W_0(t)$ vs t, i.e. $W_{k\to k}(t)$ vs t with $E_k = 0$. (**a**) For a EGOE(1 + 2) system with t up to 0.5 and the ensemble averaged results (*open symbols*) are compared with Eq. (15.9) (*continuous curves*). (**b**) For the same EGOE(1 + 2) system as in (**a**) but for t up to 2 and the ensemble averaged results (*open symbols*) are compared with theoretical results. Here, the *dashed* and *continuous curves* are obtained by using Eqs. (15.12) and (15.15) respectively. The *dotted curves* are due to Eq. (15.18). Values of the parameters in Eq. (15.18) for good fits are as follows: $\alpha = 3.5$ and $\beta = 0.6$ for $\lambda = 0.1$ and similarly, $\alpha = 17$ and $\beta = 1.36$ for $\lambda = 0.3$. (**c**) For a BEGOE(1 + 2) system and other details are same as in (**a**) except the λ values are different. (**d**) For the same BEGOE(1 + 2) system as in (**c**) and other details are as in (**b**). Here, the values of the parameters in Eq. (15.18) for good fits are as follows: $\alpha = 4$ and $\beta = 0.59$ for $\lambda = 0.04$ and similarly, $\alpha = 17$ and $\beta = 1.2$ for $\lambda = 0.1$. In all the calculation 50 member ensembles are used

15.1.3 Gaussian Region

In the Gaussian region with λ, the strength of the two-body interaction, much greater than λ_F, the strength function will be of Gaussian form. In this situation, replacing $F_k(E)$ by Gaussian form (with width σ_k) in Eq. (15.7), we obtain

$$A_{k\to k}(t) = \int_{-\infty}^{+\infty} dE \exp -iEt \frac{1}{\sqrt{2\pi}\sigma_k} \exp -\frac{(E-E_k)^2}{2\sigma_k^2}. \tag{15.13}$$

Carrying out the integral by treating 'iEt' as if it is real will give correctly the final result,

$$A_{k\to k}(t) = \exp -\left[iE_k t + \frac{\sigma_k^2 t^2}{2} \right]. \tag{15.14}$$

Therefore, for Gaussian strength functions the return probability will follow Gaussian law,

$$W_{k\to k}(t) \overset{\text{Gaussian region}}{\longrightarrow} \exp -\sigma_k^2 t^2. \tag{15.15}$$

Note that, when t is in σ_H^{-1} units, the spectral width σ_k will be in σ_H units. Thus the decay law in the BW and Gaussian regions are different in EE with $\ln W$ being linear in t for BW and quadratic for Gaussian. Some numerical examples testing Eq. (15.15) are shown in Figs. 15.1b and d for fermion and boson systems.

15.1.4 Region Intermediate to BW and Gaussian Forms for $F_k(E)$

In the BW to Gaussian transition region, as discussed in Chap. 5, it is possible to represent $F_k(E)$ by the student-t distribution defined in terms of the shape parameter α and scale parameter β as given by Eq. (5.27). With the transformations $\alpha = (\nu + 1)/2$ and $(E - E_k) = \sqrt{\frac{\beta(\nu+1)}{2\nu}}x$, the $F_k(E)$ in the transition region transforms to $F_k(x:\nu)$ where,

$$F_k(x:\nu) = \frac{\Gamma(\frac{\nu+1}{2})}{\sqrt{\pi}\sqrt{\nu}\Gamma(\frac{\nu}{2})} \frac{dx}{(\frac{x^2}{\nu}+1)^{\frac{\nu+1}{2}}}. \tag{15.16}$$

Substituting this in Eq. (15.7) gives,

$$A_{k\to k}(t) = \exp -iE_k t \int_{-\infty}^{+\infty} dx \left[\exp -i\left[\sqrt{\frac{\beta(\nu+1)}{2\nu}}t\right]x\right] F_k(x:\nu). \tag{15.17}$$

The integral in Eq. (15.17) was a subject of many investigations in statistics literature and an easily usable form was given very recently in [10]. Then the final result is,

$$\begin{aligned} &W_{k\to k}(t) \overset{\text{transition region}}{\longrightarrow} \left|A_{k\to k}(t;\nu,\beta)\right|^2; \\ &A_{k\to k}(t:\nu,\beta) = [\exp -iE_k t]\frac{2^\nu(\sqrt{\nu})^\nu}{\Gamma(\nu)} \int_0^\infty dx\left[x\left(x+\left|t'\right|\right)\right]^{(\nu-1)/2} \\ &\qquad\qquad \times \exp -\sqrt{\nu}\left(2x+\left|t'\right|\right), \\ &t' = \sqrt{\frac{\beta(\nu+1)}{2\nu}}t. \end{aligned} \tag{15.18}$$

Note that, for $\nu = 1$ we have BW form for $F_k(E)$ with $\beta = \Gamma^2/4$ and for $\nu \to \infty$ we have Gaussian form with $\sigma_k^2 = \beta/2$. Now the results in [10] and Eq. (15.18) clearly show that we will correctly recover the results given by Eqs. (15.12) and (15.15) for BW and Gaussian limits respectively. Some numerical examples testing Eq. (15.18) are shown in Figs. 15.1b and d for fermion and boson systems.

15.2 Entropy Production with Time in EGOE(1 + 2) and BEGOE(1 + 2): Cascade Model and Statistical Relaxation

Complexity generated with time can be studied by examining the time evolution of entropy. For simplicity of notation, from now on we will denote $W_{k\to f}(t)$ by $W_f(t)$ so that $W_0(t) = W_{k\to k}(t)$. Also assume that there are total $d+1$ states so that $f = 1, 2, \ldots, d$ with $|f = 0\rangle = |k\rangle$, the state in which the system is prepared at time $t = 0$. Now, entropy after time t is,

$$S_{(k)}(t) = -\sum_{f=0}^{d} W_f(t) \ln W_f(t). \tag{15.19}$$

From now on we will drop the subscript (k) in $S_{(k)}(t)$. Using Eq. (15.5), it is easy to prove the following important equality,

$$\sum_{f=0}^{d} W_f(t) = 1. \tag{15.20}$$

Before going into details of $S(t)$, let us examine $W_f(t)$. Using Eq. (15.5) we have,

$$\begin{aligned} W_f(t) &= \sum_E \left|C_0^E\right|^2 \left|C_f^E\right|^2 + 2 \sum_{E>E'} C_0^E C_f^E C_0^{E'} C_f^{E'} \cos\left(E - E'\right)t \\ &= W_f^{avg}(t) + W_f^{flu}(t). \end{aligned} \tag{15.21}$$

Note that the first term (W^{avg}) is independent of t and the second term (W^{flu}) is a fluctuating term. In three situations it is possible to simplify Eq. (15.21). First one is for $f = 0$ and we have already derived formulas for $W_0(t)$ fully taking into account both W^{avg} and W^{flu}. Next, in the small t limit we have simply

$$W_f(t) \overset{small\ t}{\longrightarrow} \left|\langle f|\exp -iHt|0\rangle\right|^2 \simeq \left|\langle f|H|0\rangle\right|^2 t^2 = H_{0f}^2 t^2. \tag{15.22}$$

Thirdly, for t large it is plausible to argue that the second term approaches zero and then $W_f(t) \approx W_f^{avg}(t)$, a constant [the first term in Eq. (15.21)]. More specifically, in the long time limit we have,

$$\begin{aligned} W_f(t) &= \sum_E \left|C_0^E\right|^2 \left|C_f^E\right|^2 \\ &\simeq \int_{-\infty}^{\infty} \frac{dE}{\rho(E)} F_0(E) F_f(E). \end{aligned} \tag{15.23}$$

In the situation that the strength functions are of BW form, one can replace $\rho(E)$ in Eq. (15.23) by its average value $\overline{\rho(E)}$ and move it outside the integral. Then, one is

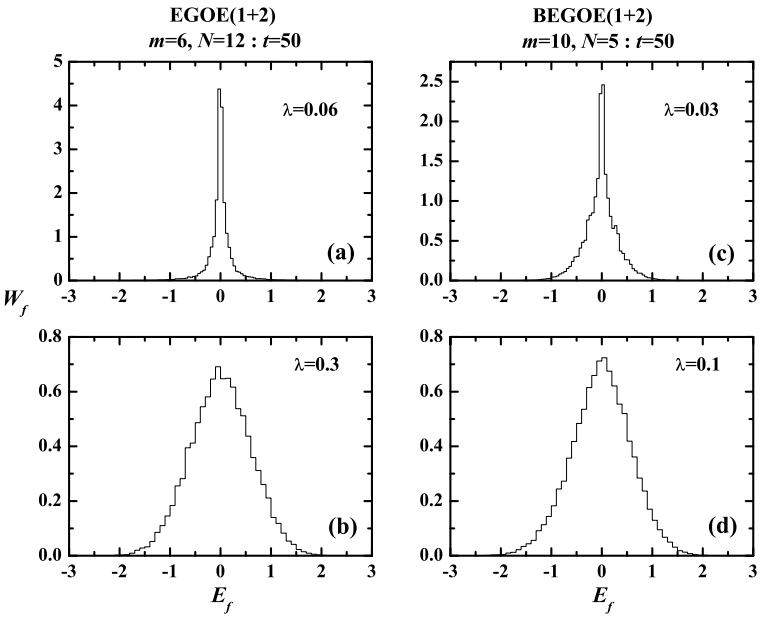

Fig. 15.2 $W_f(t)$ vs E_f for $t = 50$ value. (**a**) For a EGOE(1 + 2) system with $\lambda = 0.06$ (here BW form for strength functions applies). (**b**) For the same EGOE(1 + 2) system as in (**a**) but for $\lambda = 0.3$ (here Gaussian form for strength functions applies). (**c**) For a BEGOE(1 + 2) system with $\lambda = 0.03$ (here BW form for strength functions applies). (**d**) For the same BEGOE(1 + 2) system as in (**c**) but for $\lambda = 0.1$ (here Gaussian form for strength functions applies). In all the calculations, 25 member ensembles are used and histograms are obtained for $E_k = 0$. In the plots $\int W_f dE_f = 1$. Note that the bin sizes [see the discussion below Eq. (15.12)] used in constructing the histograms are $\Delta = 0.05$ in the BW examples and $\Delta = 0.1$ in the Gaussian examples; in all the examples $\delta = 0.005$

left with an integral that is a convolution of two BW functions giving

$$W_f(t) \simeq \frac{1}{2\pi\overline{\rho(E)}} \frac{\Gamma_t}{(E_0 - E_f)^2 + \dfrac{\Gamma_t^2}{4}}; \quad \Gamma_t = \Gamma_0 + \Gamma_f. \tag{15.24}$$

Similarly, in the situation that the strength functions are Gaussians, it is possible to evaluate the integral in Eq. (15.23) as $\rho(E)$ is a Gaussian (assumed to be zero centered with unit width) for EE. This gives,

$$W_f(t) = \frac{1}{\sqrt{\sigma_0^2 + \sigma_f^2 - \sigma_0^2\sigma_f^2}} \exp - \frac{1}{2(\sigma_0^2 + \sigma_f^2 - \sigma_0^2\sigma_f^2)} \left[(E_0 - E_f)^2 - \sigma_f^2 E_0^2 - \sigma_0^2 E_f^2\right]. \tag{15.25}$$

Figures 15.2a and b show the results for W_f vs E_f for a large value of t for EGOE(1 + 2) in BW and Gaussian regions. Similarly, Figs. 15.2c and d show the results for BEGOE(1 + 2). It is seen that the results in Fig. 15.2 are consistent with Eqs. (15.24) and (15.25). In conclusion, for large t, W_f is expected to be independent of t giving the result that entropy saturates after a large t value.

In the situation $f \neq 0$ and t is neither small or large, good knowledge of both terms in Eq. (15.21) is needed. For EE, no exact or good approximate formulas for $S(t)$ are available at present because of the complexity associated with the second term in Eq. (15.21). It is useful to note that $\sigma_k \sim \sigma_V$ and in σ_H units, it is nothing but the correlation coefficient ζ introduced in the context of NPC in EGOE(1 + 2). Also $|\langle f|\exp -iHt|0\rangle|^2$ is like strengths. Therefore, ideas based on transition strength density theory (see Chap. 5) may be useful in simplifying Eq. (15.21) in the Gaussian domain and ζ is likely to play an important role.

15.2.1 Cascade Model and Statistical Relaxation

With $S(t)$ approaching a constant as $t \to \infty$, it is important to understand the approach of $S(t)$ to saturation. As a good theory for $S(t)$ is not yet available for EE, Flambaum and Izrailev [6] introduced a Cascade model. In this model, $S(t)$ increases linearly with t. Before discussing this result, let us first consider small 't' limit result for $S(t)$. Using Eqs. (15.22) and (15.9) we have,

$$\begin{aligned} S(t) &= -W_0(t)\ln W_0(t) - \sum_f W_f(t)\ln W_f(t) \\ &\overset{small\ t}{\longrightarrow} \sigma_0^2 t^2 - t^2 \sum_{f=1}^{d} H_{0f}^2 \ln\{H_{0f}^2 t^2\}. \end{aligned} \tag{15.26}$$

Thus in the small t limit, entropy $S(t)$ will be quadratic in t.

In the cascade model of Flambaum and Izrailev [6], firstly the basis states are divided into sub-classes. The first class contains those N_1 states that are directly coupled to the initial state $|0\rangle$; i.e states for which $H_{0f} \neq 0$. The second class then contains N_2 sates that are coupled to the initial state by second order of the perturbation, i.e states for which $H_{0\alpha}H_{\alpha f} \neq 0$ with α any basis state. Continuing this cascading, let us say there are n classes. It is further assumed that all the W_f that belong to a given class will have small fluctuations and therefore, they can be replaced by their class average $\overline{W_r}$. Then $C_r = N_r\overline{W_r}$ and $\sum_0^\infty C_r = 1$. As N_n is expected to grow with n, one may put $N_n \approx M^n$ with M some constant. As N_n grows with n, this justifies neglecting the return probability to the previous classes and then (assuming BW form for strength functions),

$$\frac{dC_r}{dt} = -\Gamma\{C_r - C_{r-1}\}. \tag{15.27}$$

The first term here is the probability for the system to be in class r and the second term is the flux from the previous class. Solution of Eq. (15.27) is

$$C_r = \frac{(\Gamma t)^r}{r!} \exp -\Gamma t. \tag{15.28}$$

Assuming infinite number of classes, we have the identity $\sum_{r=0}^{\infty} C_r = 1$. Now, the entropy after time t is

$$\begin{aligned} S_0(t) &\approx -\sum_{r=0}^{\infty} C_r \ln\left(\frac{C_r}{N_r}\right) \\ &= -\sum_{r=0}^{\infty} \frac{(\Gamma t)^r}{r!} [\exp -\Gamma t] \left\{ -r \ln M - \Gamma t + \ln \frac{(\Gamma t)^r}{r!} \right\} \\ &= t\big[\Gamma(1 + \ln M)\big] - \left[(\exp -\Gamma t) \sum_{r=0}^{\infty} \frac{(\Gamma t)^r}{r!} \ln \frac{(\Gamma t)^r}{r!} \right]. \end{aligned} \tag{15.29}$$

In the last equality, the second term on the right-hand side is much smaller than the first term giving

$$S_0(t) \approx t\Gamma \ln M. \tag{15.30}$$

For Gaussian strength functions it is plausible to use Eq. (15.30) by replacing Γ by σ_0. Most important observation that follows from Eq. (15.30) is that the entropy after a small time will increase linearly with t. Thus it is expected, in the BW and Gaussian domains of EE, that with increasing time, the entropy will have initial quadratic growth as given by perturbation theory, then the linear behavior as given by the cascade model and finally saturation (saturation value will be the GOE value $\ln 0.48 d_{eff}$ where d_{eff} is an 'effective' dimension). Numerical results for EGOE(1 + 2) and BEGOE(1 + 2) are shown in Figs. 15.3a–d and they exhibit the expected behavior. For more quantitative description, it is possible to use Eqs. (15.19) and (15.20) with the assumption that in the sum only f's in an energy shell will contribute and within the shell, the variation of $W_f(t)$ is small. Then, with N_s the number of f's inside the energy shell, we have

$$S_0(t) = -W_0(t) \ln W_0(t) - \big[1 - W_0(t)\big] \ln\left(\frac{1 - W_0(t)}{N_s}\right). \tag{15.31}$$

The N_s in Eq. (15.31) can be determined numerically from $N_s \sim \langle \exp S \rangle$ where the average can be taken over a long time interval. This and Eq. (15.31) give a good description of the numerical results in Fig. 15.3. Equation (15.31) is expected to be good when the number of classes n is small. This appears to be true in practice as shown in some examples in [2]. Note that the condition $dW_n/dt = 0$ gives $n = \Gamma t$ (therefore for $t \ll 1/\Gamma$, there will be flow only into the first class). Another important observation is that in the BW region, $S(t)$ exhibits oscillations after the

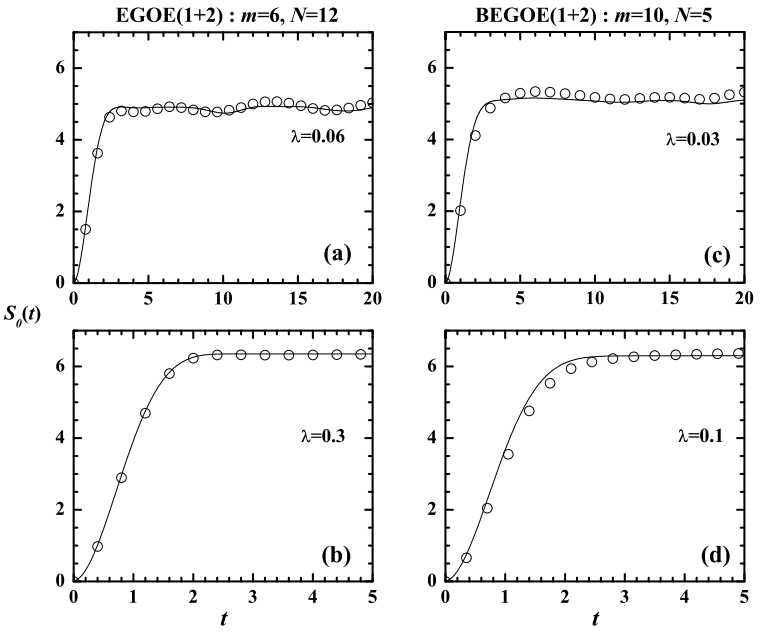

Fig. 15.3 Entropy $S_0(t)$ vs t for k states with $E_k = 0$ for EGOE(1 + 2) and BEGOE(1 + 2) examples. Ensemble averaged numerical results (*open circles*) are compared with the results from Eq. (15.31). See Fig. 15.2 for further details

linear increase. Flambaum and Izrailev [6] gave an explanation for this result but there is no formal derivation yet for this.

It is useful to add that interacting spin 1/2 fermions or hard-core bosons on 1D lattice and bosons on a 1D ring are also shown [2, 4] to exhibit statistical relaxation [$S_0(t)$ vs t behavior] similar to the results for spinless EE shown in Fig. 15.3. Going beyond these systems, it will be useful to study in future the role of spin in statistical relaxation by analyzing spin ensembles described in Chaps. 6 and 10.

15.3 Ergodicity Principle for Expectation Values of Observables: EGOE(1 + 2) Results

In recent years, study of the equilibration and thermalization mechanisms in isolated finite quantum systems has attracted great interest partly because the non-equilibrium dynamics, after an external perturbation is applied, has become experimentally accessible for ultra-cold quantum gases and electrons in mesoscopic systems such as quantum dots [11–13]. Advances in technology makes it possible to induce sharp changes in the parameters controlling the system and then observe the subsequent time evolution, which is essentially unitary because on short and intermediate time scales the perturbed system is almost isolated from the environment.

Thus, one can experimentally study if an isolated system, after a sharp perturbation, thermalizes or retains memory of the initial conditions. Here, it seems that the so-called eigenstate thermalization hypothesis (ETH) [14, 15] plays a fundamental role. The ETH states that thermalization occurs at the level of individual eigenstates whenever they satisfy Berry's conjecture [16] on chaotic eigenfunctions, i.e., whenever they behave as (quasi) random superpositions of the basis states. For this and other reasons, the role played by quantum chaos and chaotic wavefunctions in thermalization has been investigated using some 1D and 2D fermionic and bosonic systems by Rigol and others [2, 17–21].

In another line of approach, the EGOE(1 + 2), BEGOE(1 + 2) and their spin versions, as described in Chaps. 5, 6, 9 and 10, have been used, together with some related models, such as nuclear shell model, to perform different studies on thermalization of isolated fermionic and bosonic systems. As already discussed in the previous chapters and in the reviews [22, 23], the thermalization criteria used in these studies were based on the equivalence between different definitions of entropy, different definitions of temperature and representability of occupancies by Fermi-Dirac distribution (Bose-Einstein distribution for bosons). There are also some calculations of expectation values using the canonical distribution [24]. However, to get a deeper understanding of the role of quantum chaos, it is important that the ergodicity principle [25, 26], which is the cornerstone for thermalization, and clearly more precise and general than the aforementioned criteria, is tested. Here below, we will present the results from a EGOE(1 + 2) study of ergodicity principle using expectation values of operators.

15.3.1 Long-Time Average and Micro-canonical Average of Expectation Values

Let us begin with EGOE(1 + 2) for m spinless fermions in N sp states as in Sect. 15.1 with H defined by Eq. (15.1). Say EGOE(1 + 2) generates eigenvalues E_μ, $\mu = 1, 2, \ldots, d$ where the dimension $d = \binom{N}{m}$. Further let us introduce the following notations,

$$\begin{aligned} \Delta E_{\mu,\nu} &= E_\nu - E_\mu, \\ D_\mu(\mathscr{O}) &= \langle E_\mu|\mathscr{O}|E_\mu\rangle, \\ R_{\mu,\nu}(\mathscr{O}) &= \langle E_\mu|\mathscr{O}|E_\nu\rangle, \quad \mu \neq \nu. \end{aligned} \tag{15.32}$$

Now, consider a quantum system modeled by EGOE(1 + 2) and prepared at time $t = 0$ in the state $|\Psi(0)\rangle$. Say that this state is localized in a 'narrow' energy window around energy E,

$$\Psi(0) = \sum_\mu{}' C_\mu |E_\mu\rangle. \tag{15.33}$$

In order to make this precise, we need models for C_μ and we will return to this later. The system is said to thermalizes if the long time average of 'any reasonable observable' $\mathscr{O}$

$$\langle \mathscr{O} \rangle^t_{\Delta t} = \frac{1}{2\Delta t} \int_{t-\Delta t}^{t+\Delta t} \big\langle \Psi(t) \big| \mathscr{O} \big| \Psi(t) \big\rangle, \tag{15.34}$$

converges to a constant value predictable by an appropriate statistical ensemble, like for example micro-canonical ensemble. Using the time evolution of the eigenstates, as discussed in the previous two sections, we can introduce the density operators $\rho(\Psi, t)$, $\rho_D(\Psi)$ and $\rho_{ND}(\Psi, t)$,

$$\begin{aligned} \rho(\Psi, t) &= \big| \Psi(t) \big\rangle \big\langle \Psi(t) \big| \\ &= \sum_\mu |C_\mu|^2 |E_\mu\rangle\langle E_\mu| + \sum_{\mu \neq \nu}^{1,2,\ldots,d} C^*_\mu C_\nu \exp\left\{ \frac{i}{\hbar} \Delta E_{\mu,\nu} t \right\} |E_\mu\rangle\langle E_\nu| \\ &= \rho_D(\Psi) + \rho_{ND}(\Psi, t) \end{aligned} \tag{15.35}$$

and then, the expectation value of an operator $\mathscr{O}$ is

$$\big\langle \Psi(t) \big| \mathscr{O} \big| \Psi(t) \big\rangle = \big\langle\!\big\langle \mathscr{O} \rho(\Psi, t) \big\rangle\!\big\rangle = \big\langle\!\big\langle \mathscr{O} \rho_D(\Psi) \big\rangle\!\big\rangle + \big\langle\!\big\langle \mathscr{O} \rho_{ND}(\Psi, t) \big\rangle\!\big\rangle. \tag{15.36}$$

If we consider long time average of the expectation values, the second term in Eq. (15.36) will tend to zero, i.e. the non-diagonal term vanishes. This is seen as follows,

$$\begin{aligned} \frac{1}{2\Delta t} \int_{t-\Delta t}^{t+\Delta t} \big\langle\!\big\langle \mathscr{O} \rho_{ND}(\Psi, t) \big\rangle\!\big\rangle \quad &= \quad \sum_{\mu \neq \nu}^{1,2,\ldots,d} C^*_\mu C_\nu R_{\mu,\nu}(\mathscr{O}) \frac{1}{2\Delta t} \\ &\quad \times \int_{t-\Delta t}^{t+\Delta t} \exp\left\{ \frac{i}{\hbar} \Delta E_{\mu,\nu} t' \right\} dt'; \\ \frac{1}{2\Delta t} \int_{t-\Delta t}^{t+\Delta t} \exp\left\{ \frac{i}{\hbar} \Delta E_{\mu,\nu} t' \right\} dt' \quad &= \quad \exp\left\{ \frac{i}{\hbar} \Delta E_{\mu,\nu} t \right\} \frac{\sin[\Delta E_{\mu,\nu} \Delta t/\hbar]}{[\Delta E_{\mu,\nu} \Delta t/\hbar]}, \\ \frac{\sin[\Delta E_{\mu,\nu} \Delta t/\hbar]}{[\Delta E_{\mu,\nu} \Delta t/\hbar]} &\overset{\Delta t \gg 1}{\sim} 0. \end{aligned} \tag{15.37}$$

Therefore the long time average $(t - av)$ gives the diagonal approximation,

$$\langle \mathscr{O} \rangle_{t-av} \overset{\Delta t \gg 1}{\sim} \big\langle\!\big\langle \mathscr{O} \rho_D(\Psi) \big\rangle\!\big\rangle = \sum_\mu |C_\mu|^2 D_\mu(\mathscr{O}) = \sum_\mu |C_\mu|^2 \langle E_\mu | \mathscr{O} | E_\mu \rangle. \tag{15.38}$$

It is easy to see that we can write the last form in terms of the 'strength function' $F_{\Psi(0)}(E)$ and the expectation value density $\rho_{\mathscr{O}}(E_\mu) = \langle E_\mu | \mathscr{O} | E_\mu \rangle \rho(E_\mu)$.

For isolated systems, micro-canonical ensemble is expected to be more appropriate. Then, the ensemble averaged expectation value is obtained by averaging the

expectation value $\langle E_\mu|\mathscr{O}|E_\mu\rangle$ in a energy window $E_0 \pm \Delta E$. The ΔE is sufficiently small compared to the spectrum span but large enough to contain many eigenstates [note that level (and strength) fluctuations over the window $E_0 \pm \Delta E$ average out]. With say d' levels in the energy shell $W = \{|E_\mu\rangle;\, E_\mu \in [E_0 - \Delta E, E_0 + \Delta E]\}$, this gives ρ_{stat} where

$$\rho_{stat} = \frac{1}{d'} \sum_{\mu}^{'} |E_\mu\rangle\langle E_\mu|. \tag{15.39}$$

The symbol Σ' means the sum is restricted to eigenstates belonging to W. Then the corresponding micro-canonical average is,

$$\langle \mathscr{O} \rangle_{stat} = \frac{1}{d'} \sum_{E_\mu = E_0 - \Delta E}^{E_0 + \Delta E} \langle E_\mu|\mathscr{O}|E_\mu\rangle. \tag{15.40}$$

For thermalization, we need

$$\langle \mathscr{O} \rangle_{t-av} \approx \langle \mathscr{O} \rangle_{stat}. \tag{15.41}$$

To find the region of thermalization in EGOE(1 + 2) (essentially checking the goodness of the λ_t marker determined in Chaps. 5, 6 and 9), the following measure $\Delta_{\mathscr{O}}$ has been considered in [3],

$$\Delta_{\mathscr{O}} = \left| \frac{\langle \mathscr{O} \rangle_{t-av} - \langle \mathscr{O} \rangle_{stat}}{\langle \mathscr{O} \rangle_{stat}} \right| \tag{15.42}$$

and then

$$\Delta_{\mathscr{O}} \approx 0 \tag{15.43}$$

corresponds to thermalization.

15.3.2 Thermalization from Expectation Values

In order to verify $\Delta_o \to 0$ in some limit, four types of operators are considered in [3]:

- diagonal one-body operators $\mathscr{O}_d(1) = \sum_k \theta_k a_k^\dagger a_k$,
- general one-body operators $\mathscr{O}(1) = \sum_{k,l} \theta_{kl} a_k^\dagger a_l$,
- general two-body operators $\mathscr{O}(2) = \sum_{k<l,p<q} \theta_{klpq} a_k^\dagger a_l^\dagger a_q a_p$,
- strength function operators $\mathscr{O}_{sf} = \mathscr{O}^T(1)\mathscr{O}(1)$,

where the parameters θ_k, θ_{kl} and θ_{klpq} are taken as random variables. To see how the initial conditions affect thermalization process, the system has been allowed to evolve from three different types of initial states, defined as:

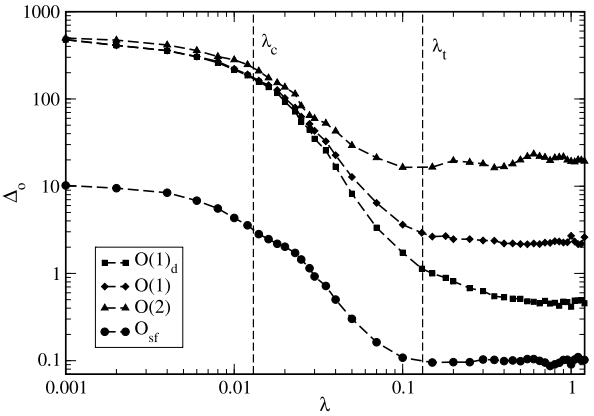

Fig. 15.4 Variation with the interaction strength λ of the ensemble averaged $\Delta_{o_d(1)}$ (*squares*), $\Delta_{o(1)}$ (*diamonds*), $\Delta_{o(2)}$ (*triangles*), and $\Delta_{o_{sf}}$ (*dots*), given in percent, for a 60 member EGOE(1 + 2) with $(m, N) = (6, 16)$ initially prepared in a state $\Psi^{(1)}(0) \in W$. Figure is taken from [3] with permission from IOP publishing

- $|\Psi^{(1)}(0)\rangle \propto P_W|k_0\rangle$, where P_W is the projector onto W, and $|k_0\rangle$ is the mean-field state with energy E_0.
- $|\Psi^{(2)}(0)\rangle \propto \sum_\mu^{'} C_\mu|E_\mu\rangle$, with the coefficients C_μ being $G(0, 1)$ variables.
- $|\Psi^{(3)}(0)\rangle \propto \sum_\mu^{'} C_\mu|E_\mu\rangle$, where $C_\mu = \exp\{-\alpha(\frac{E_\mu - E_0}{\Delta E})^2\}\ G(0, 1)$.

The states $\Psi^{(2)}(0)$ and $\Psi^{(3)}(0)$ are random superpositions of the eigenstates belonging to W, but due to the Gaussian factor the distribution of the C_μ coefficients is wider for $\Psi^{(3)}(0)$. As we shall see below, distribution of the state amplitudes inside W is one of the factors that affects the thermalization process. In the calculations, W is chosen such that $E_0 = 0$ and $\Delta E = 0.1$ (all energies being zero centered and normalized to unit spectral width).

In the EGOE(1 + 2) calculations carried out, the sp energies ϵ_k are chosen to be independent Gaussian variables with $\overline{\epsilon_k} = k$ and $\overline{(\epsilon_k - k)^2} = 1/2$. Figure 15.4 shows the results for $\Delta_{\mathscr{O}}$ for the four operators as a function of the interaction strength λ for a 60 member EGOE(1 + 2) with $(m, N) = (6, 16)$ (matrix dimension being 8008). In the figure, the two vertical lines give the positions of λ_c and λ_t. In all the cases $\Delta_{\mathscr{O}}$ becomes smaller as the interaction strength increases up to $\lambda \approx \lambda_t$. It is very important to realize that the transition from Poisson to GOE spectral fluctuations, which is considered the most relevant signature of quantum chaos, occurs at $\lambda \approx \lambda_c$ and does not modify this trend. On the contrary, for $\lambda > \lambda_t$ the relative errors either remain essentially constant or the decreasing rate is much smaller. Recall that λ_t defines a region where the three entropies S^{ther}, S^{info} and S^{sp} take essentially the same values, and signals the point at which the wave functions start becoming very much delocalized in the mean-field basis. Beyond λ_t, $\Delta_{\mathscr{O}}$ becomes clearly smaller than one percent only for two operators, namely $\mathscr{O}_d(1)$ and $\mathscr{O}_{sf}$. Their errors are ≈0.5 % and ≈0.1 %, respectively. Thus, as long as the system is prepared in an initial state $\Psi^{(1)}(0) \in W$ and $\lambda > \lambda_t$, Eq. (15.41) approximately holds for the observables $\mathscr{O}_d(1)$ and $\mathscr{O}_{sf}$. Thus the system thermalizes relative to these two observables. This is not the case of the observables $\mathscr{O}(1)$ and $\mathscr{O}(2)$. It is worth noting that the main difference between $\mathscr{O}(1)$, $\mathscr{O}(2)$ in one hand, and $\mathscr{O}_d(1)$, $\mathscr{O}_{sf}$ in the other, is that the latter have meaningful smoothed form for large λ, as discussed in Chap. 5.

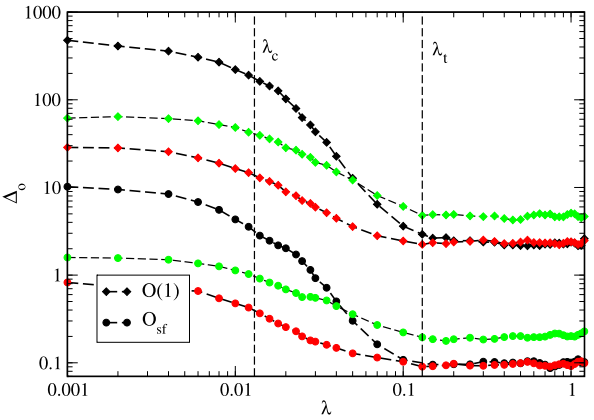

Fig. 15.5 Values of ensemble averaged $\Delta_{o(1)}$ (*diamonds*) and $\Delta_{o_{sf}}$ (*dots*), expressed in percent, as function of λ for a 60 member EGOE(1 + 2) with $(m, N) = (6, 16)$, and initial conditions given by $\Psi^{(1)}(0)$ (*black*), $\Psi^{(2)}(0)$ (*red*), and $\Psi^{(3)}(0)$ (*green*). In all cases the initial state belongs to the energy shell W. Figure is taken from [3] with permission from IOP publishing

The results corresponding to other choices of $\Psi(0) \in W$ are shown in Fig. 15.5. For simplicity, results are shown only for $\mathscr{O}_{sf}$ and $\mathscr{O}(1)$. Curves in black, red and green correspond to $\Psi^{(1)}(0)$, $\Psi^{(2)}(0)$ and $\Psi^{(3)}(0)$, respectively. In all cases the initial state belongs to the energy shell W. We see that the choice of the initial conditions does not affect the main trend: $\Delta_{o(1)}$, and $\Delta_{o_{sf}}$ diminish progressively as the strength λ is increased, and for $\lambda > \lambda_t$ their values remain essentially constant. However, the precise values are quite different. When $\lambda > \lambda_t$, the initial states $\Psi^{(1)}(0)$ and $\Psi^{(2)}(0)$ give rise to very similar results while the error corresponding to $\Psi^{(3)}(0)$ is clearly larger. Moreover, as in Fig. 15.4, expectation values of the operator $\mathscr{O}(1)$ do not thermalize independent of the initial condition while $\mathscr{O}_{sf}$ thermalizes.

In order to obtain some analytical insight into the behavior of $\Delta_{\mathscr{O}}$, it is plausible to consider C_μ to be Gaussian random variables lying on a unit sphere in W. Then the fluctuation properties of C_μ follow P-T law and $\overline{|C_\mu|^2} = 1/d'$. Also, it is possible to assume that C_μ and $A_\mu = \langle E_\mu|\mathscr{O}|E_\mu\rangle$ are independent. Then clearly,

$$|\Delta_{\mathscr{O}}|^2 = \frac{\overline{\{\sum_{\mu=1}^{d'}(|C_\mu|^2 - \frac{1}{d'})A_\mu\}^2}}{[\{\frac{1}{d'}\sum_{\mu=1}^{d'} A_\mu\}]^2} = \frac{2}{d'}\frac{\frac{1}{d'}\sum_{\mu=1}^{d'}\overline{(A_\mu - \overline{A_\mu})^2}}{[\{\frac{1}{d'}\sum_{\mu=1}^{d'} A_\mu\}]^2}. \tag{15.44}$$

For $\mathscr{O} = \mathscr{O}_{sf} = \mathscr{O}^T(1)\mathscr{O}(1)$, the factor multiplying $\frac{2}{d'}$ in Eq. (15.44) is nothing but the inverse of the NPC in transition strengths ($\xi^{(s)}_{2:\mathscr{O}(1)}$) generated by the one-body operator $\mathscr{O}(1)$. This result is discussed in Sect. 5.5 with the final result following from Eq. (5.48),

$$|\Delta_{\mathscr{O}}| = \sqrt{\frac{4}{3d'}}\left[\xi^{(s)}_{2:\mathscr{O}(1)}(E_0)\right]^{-1/2}. \tag{15.45}$$

This establishes a connection between the thermalization of the system, relative to an observable $\mathscr{O}_{sf} = \mathscr{O}^T(1)\mathscr{O}(1)$, and the value of the NPC for the transition strengths generated by $\mathscr{O}(1)$ acting on the eigenstate with energy E_0. An important outcome is that for chaotic systems the NPC is expected to be large and hence these systems will thermalize, while for regular systems NPC has to be small and thus thermalization will be hindered. More details of EGOE(1 + 2) study of thermalization using expectation values is given in [3].

In summary, it is found that the λ_t marker indeed marks the region of thermalization and thermalization occurs only for certain types of operators such as occupancies (and their linear combinations) and strength function operators. It is also seen in the numerical calculations (by varying W value) that spectrum edges hinder thermalization and also large Hilbert space enhances thermalization process.

Before concluding this chapter, it should be added that besides the first studies on statistical relaxation and thermalization using EGOE(1 + 2) [also BEGOE(1 + 2)], there is also an attempt by Seligman et al. [5] to study Loschmidt echoes in EGOE(1 + 2). Their study showed that the fidelity amplitude displays 'freeze'. This freeze, typically present for most realizations (most members) of EGOE(1 + 2), is found to vanish on average. More detailed studies of this may give new information on the ergodic properties of EGOE(1 + 2).

References

1. V.V. Flambaum, Time dynamics in chaotic many-body systems: can chaos destroy a quantum computer? Aust. J. Phys. **53**, 489–497 (2000)
2. L.F. Santos, F. Borgonovi, F.M. Izrailev, Onset of chaos and relaxation in isolated systems of interacting spins: energy shell approach. Phys. Rev. E **85**, 036209 (2012)
3. V.K.B. Kota, A. Relaño, J. Retamosa, M. Vyas, Thermalization in the two-body random ensemble, J. Stat. Mech. P10028 (2011)
4. G.P. Berman, F. Borgonovi, F.M. Izrailev, A. Smerzi, Irregular dynamics in a one-dimensional Bose system. Phys. Rev. Lett. **92**, 030404 (2004)
5. I. Pižorn, T. Prosen, T.H. Seligman, Loschmidt echoes in two-body random matrix ensembles. Phys. Rev. B **76**, 035122 (2007)
6. V.V. Flambaum, F.M. Izrailev, Entropy production and wave packet dynamics in the Fock space of closed chaotic many-body systems. Phys. Rev. E **64**, 036220 (2001)
7. V.K.B. Kota, R. Sahu, Structure of wavefunctions in (1 + 2)-body random matrix ensembles. Phys. Rev. E **64**, 016219 (2001)
8. M. Abramowtiz, I.A. Stegun (eds.), *Handbook of Mathematical Functions*, NBS Applied Mathematics Series, vol. 55 (U.S. Govt. Printing Office, Washington, D.C., 1972)
9. A. Bohr, B.R. Mottelson, *Nuclear Structure*, Single-Particle Motion, vol. I (Benjamin, New York, 1969)
10. I. Dreier, S. Kotz, A note on the characteristic function of the t-distribution. Stat. Probab. Lett. **57**, 221–224 (2002)
11. R. Jördens, N. Strohmaier, K. Günter, H. Moritz, T. Esslinger, A Mott insulator of fermionic atoms in an optical lattice. Nature **455**, 204–207 (2008)
12. U. Schneider et al., Metallic and insulating phases of repulsively interacting fermions in a 3D optical lattice. Science **322**, 1520–1525 (2008)
13. L. Perfetti et al., Time evolution of the electronic structure of 1T-TaS2 through the insulator-metal transition. Phys. Rev. Lett. **97**, 067402 (2006)

14. M. Srednicki, Chaos and quantum thermalization. Phys. Rev. E **50**, 888–901 (1994)
15. J.M. Deutsch, Quantum statistical mechanics in a closed system. Phys. Rev. A **43**, 2046–2049 (1991)
16. M.V. Berry, Regular and irregular semiclassical wavefunctions. J. Phys. A **10**, 2083–2091 (1977)
17. M. Rigol, V. Dunjko, M. Olshanii, Thermalization and its mechanism for generic isolated quantum systems. Nature (London) **452**, 854–858 (2008)
18. M. Rigol, Breakdown of thermalization in finite one-dimensional systems. Phys. Rev. Lett. **103**, 100403 (2009)
19. L.F. Santos, M. Rigol, Onset of quantum chaos in one dimensional bosonic and fermionic systems and its relation to thermalization. Phys. Rev. E **81**, 036206 (2010)
20. L.F. Santos, M. Rigol, Localization and the effects of symmetries in the thermalization properties of one-dimensional quantum systems. Phys. Rev. E **82**, 031130 (2010)
21. L.F. Santos, F. Borgonovi, F.M. Izrailev, Chaos and statistical relaxation in quantum systems of interacting particles. Phys. Rev. Lett. **108**, 094102 (2012)
22. V.K.B. Kota, Embedded random matrix ensembles for complexity and chaos in finite interacting particle systems. Phys. Rep. **347**, 223–288 (2001)
23. J.M.G. Gómez, K. Kar, V.K.B. Kota, R.A. Molina, A. Relaño, J. Retamosa, Many-body quantum chaos: recent developments and applications to nuclei. Phys. Rep. **499**, 103–226 (2011)
24. V.V. Flambaum, A.A. Gribakina, G.F. Gribakin, I.V. Ponomarev, Quantum chaos in many-body systems: what can we learn from the Ce atom. Physica D **131**, 205–220 (1999)
25. P. Reimann, Foundation of statistical mechanics under experimentally realistic conditions. Phys. Rev. Lett. **101**, 190403 (2008)
26. S. Goldstein, J.L. Lebowitz, C. Mastrodonato, R. Tumulka, N. Zanghi, Approach to thermal equilibrium of macroscopic quantum systems. Phys. Rev. E **81**, 011109 (2010)